https://doi.org/10.5194/tc-2020-50
Preprint. Discussion started: 17 February 2020

The Cryosphere Discussions
Open Access
EGU

A simple model of mélange buttressing for calving glaciers

Tanja Schlemm[1,2] and Anders Levermann[1,2,3]

[1]Potsdam Institute for Climate Impact Research, Potsdam, Germany
[2]Institute of Physics and Astronomy, University of Potsdam, Potsdam, Germany
[3]Lamont-Doherty Earth Observatory, Columbia University, New York, USA

Correspondence: anders.levermann@pik-potsdam.de

Abstract. Both ice sheets on Greenland and Antarctica are discharging ice into the ocean. In many regions along the coast of the ice sheets, the icebergs calf into a bay. If the addition of icebergs through calving is faster than their transport out of the embayment, the icebergs will be frozen into a mélange with surrounding sea ice in winter. In this case, the buttressing effect of the ice mélange can be considerably stronger than any buttressing by mere sea ice would be. This in turn stabilizes the glacier terminus and leads to a reduction in calving rates. Here we propose a simple but robust ~~buttressing model~~ of ice mélange which can be used in numerical and analytical modeling.

1 Introduction

Ice sheets gain mass by snowfall and freezing of sea water and lose mass through calving of icebergs and melting at the surface and the bed. Currently the ice sheets on Antarctica and Greenland have a net mass loss and contribute increasingly to sea level rise (Rignot et al., 2014; Shepherd et al., 2018; WCRP Global Sea Level Budget Group, 2018; Eric Rignot, 2019; Mouginot et al., 2019). The ice sheet's future mass loss is important for sea level projections (Church et al., 2013; Ritz et al., 2015; Golledge et al., 2015; DeConto and Pollard, 2016; Mengel et al., 2016; Kopp et al., 2017; Slangen et al., 2017; Golledge et al., 2019; Levermann et al., 2019).

For the Greenland ice sheet, calving accounted for two-thirds of the ice loss between 2000 and 2005, while the rest was lost due to enhanced surface melting (Rignot and Kanagaratnam, 2006). Because surface melt increased faster than glacier speed, calving was responsible for a third of the mass loss of the Greenland ice sheet between 2009 and 2012 (Enderlin et al., 2014). In the future, enhanced warming (Franco et al., 2013) and the melt elevation feedback (Levermann and Winkelmann, 2016) will further increase surface melt but also intensify the flow of ice into the ocean. Calving accounts for roughly half the ice loss of the Antarctic ice shelves, the rest is lost by basal melt (Depoorter et al., 2013).

It is clear that calving plays an important role in future ice loss. However, by just calving off icebergs into the ocean and considering them eliminated from the stress field of the ice-sheet-ice-shelf system, most studies neglect the buttressing effect

https://doi.org/10.5194/tc-2020-50
Preprint. Discussion started: 17 February 2020

of a possible ice mélange, which can form within the embayment into which the glacier is calving. This study provides a simple parametrization that accounts for the buttressing effect of ice mélange on calving on a large spatial scale and that can be used for continental scale ice sheet modeling. Such simulations are typically run on resolutions of several kilometres and over decadal to millennial timescales.

Any melange parameterization needs to be combined with a large-scale calving parameterizations of which there are some. Benn et al. (2007) proposed a crevasse-depth calving-criterion assuming that once a surface crevasse has reached the water level, an iceberg calves off. This does not give a calving rate but rather the position of the calving front with the assumption that ice in front calved off. It has been implemented in a flow-line model by Nick et al. (2010). Levermann et al. (2012) proposed a strain rate dependent calving rate for ice shelves. Morlighem et al. (2016) proposed a calving rate parametrization based on von Mises stress and glacier flow veloctiy. Mercenier et al. (2018) derived a calving rate for a grounded glacier based on tensile failure.

In addition to calving caused by crevasses, another calving mechanism called cliff calving has first been proposed by Bassis and Walker (2011), who found that ice cliffs with a freeboard (ice thickness minus water depth) larger than $100\,\mathrm{m}$ are inherently unstable due to shear failure. Cliff calving was implemented as an almost step-like calving rate by Pollard et al. (2015); DeConto and Pollard (2016), while Bassis et al. (2017) implemented cliff calving as a criterion for the calving front position. Finally, Schlemm and Levermann (2019) derived a cliff calving rate dependent on glacier freeboard and water depth by analyzing stresses close to the glacier terminus and using a Coulomb failure criterion.

Melange buttressing is likely to have a stabilizing effect on possible ice sheet instabilities. First the so-called Marine Ice Sheet Instability (MISI) (Mercer, 1978; Schoof, 2007; Favier et al., 2014) which can unfold if the grounding line is situated on a reverse-sloping bed. Secondly, if the ice shelves buttressing the grounding line have disintegrated due to calving or melting and large ice cliffs become exposed, runaway cliff calving might lead to the Marine Ice Cliff Instability (MICI) (Pollard et al., 2015). DeConto and Pollard (2016) carried out past and future simulations of the Antarctic ice sheet with cliff calving implemented as a step function with a discussed but rather ad-hoc upper limit of $3\,\mathrm{km/a}$ as well as an additional hydrofracturing process that attacks the ice shelves. Edwards et al. (2019) did further analysis with upper limits between $1-10\,\mathrm{km/a}$. The simulations were compared to mid-Pliocene ice retreat (about 3 million years ago), where sea level was $5-20\,\mathrm{m}$ higher than present day. Given the uncertainty in many ice sheet parameters as well as uncertainties in air and ocean temperature forcing, agreement between simulations and observations could be achieved even without MICI. Calving rates larger than $10\,\mathrm{km/a}$ were not considered, but it is clear that using one of the recently derived calving parametrisations with calving rates up to at least $65\,\mathrm{km/a}$ (see fig. 1) would result in too much and too fast ice retreat. An upper limit on the calving rates appears to be necessary.

So far, the calving rate cutoff has been an ad-hoc assumption. However, this upper limit should correspond to some physical process that is responsible for limiting calving rates. We propose that ice mélange, a mix of icebergs and sea ice that is found in many glacial embayments, gives rise to a negative feedback on calving rates.

https://doi.org/10.5194/tc-2020-50
Preprint. Discussion started: 17 February 2020

The Cryosphere Discussions
Open Access
EGU

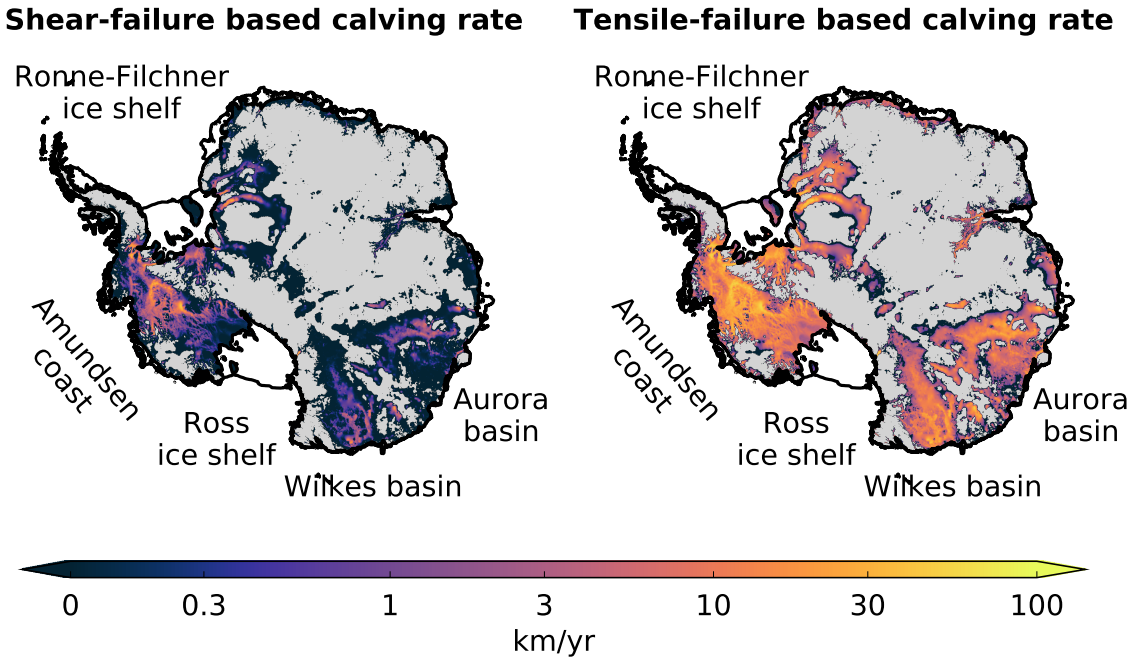

Figure 1. Potential shear-failure based calving rates (eq. 9) and tensile-failure based calving rates (eq. 8) in the grounded, marine regions of the Antarctic ice sheet. Floating ice is shown in white and grounded ice above sea level in grey. In the marine regions, ice is assumed to be at floatation thickness, which gives a minimal estimate of the potential calving rates. Estimates for shear calving rates go up to 65 km/a and estimates for tensile calving rates go up to 75 km/a. If the grounding line retreat is faster than the speed with which the glacier terminus thins to floatation, calving rates could be even larger. Imposing an upper bound on the calving rates is necessary to prevent unrealistic, runaway ice loss.

Obeservations in Store glacier and Jakobshavn glacier in Greenland have shown that in the winter, when sea ice is thick, ice mélange prevents calving (Walter et al., 2012; Xie et al., 2019). This has also been reproduced in modelling studies of grounded marine glaciers (Krug et al., 2015; Todd et al., 2018, 2019): Backstresses from the mélange reduce the stresses in the glacier terminus thereby limiting crevasse propagation and reducing calving rates or preventing calving completely. There's a large uncertainty in the value of mélange backstresses, values given in the literature range between $0.02 - 3$ MPa (Walter et al., 2012; Krug et al., 2015; Todd et al., 2018). Burton et al. (2018) have shown that the mélange backstress increases with L/W, the ratio of mélange length to the width of confining channel. The presence of pinning points where the mélange grounds can also increase the backpressure. Seasonality of basal melting and resulting thinning of the ice mélange is another important parameter for mélange backstress.

In addition to the reduced stresses caused by the backstress of the mélange, the presence of mélange prevents a full-thickness ice berg from rotating away from the terminus, even more so if the glacier is thicker than floatation thickness (Amundson et al., 2010). Tensile-failure based calving (Mercenier et al., 2018) is likely to produce full thickness icebergs and may be hindered

https://doi.org/10.5194/tc-2020-50
Preprint. Discussion started: 17 February 2020


The Cryosphere Discussions

significantly by mélange. Shear-failure based calving (Schlemm and Levermann, 2019) is more likely to produce many smaller icebergs (breakup occurs through many small, interacting fractures at the foot of the terminus) and might be less influenced by mélange.

Ice mélange is also relevant for calving from shelves in Antarctica: the presence of mélange stabilizes rifts in the ice shelf and can prevent tabular icebergs from separating from the iceshelf (Rignot and MacAyeal, 1998; Khazendar et al., 2009; Jeong et al., 2016).

We propose a negative feedback between calving rate and mélange thickness: A glacier terminus with high calving rates produces a lot of icebergs, which become part of the ice mélange in front of the glacier. The ~~thicker~~ the mélange is, the stronger it buttresses the glacier terminus leading to reduced calving rates.

In section 2, we will show that with a few simple assumptions, this negative feedback between calving rate and mélange thickness leads to an upper limit on the calving rates. Application to two calving parametrizations and possible simplifications are discussed in section 3. Section 4 applies the mélange buttressed calving rates to an idealized glacier setup.

2 Derivation of an upper limit to calving rates due to mélange buttressing

Mélange can prevent calving in two ways: First, in the winter, additional sea ice stiffens and forcifies the mélange and can thus inhibit calving for example of Greenland glaciers (Amundson et al., 2010; Todd and Christoffersen, 2014; Krug et al., 2015). Secondly, a weaker mélange can still prevent a full-thickness iceberg from rotating out (Amundson et al., 2010) and thus prevent further calving.

Ice sheet models capable of simulating the whole Greenland or Antarctic ice sheet over decadal to millennial timescales cannot resolve the stresses at individual calving glacier termini and often do not resolve seasonal variations in forcing. Therefore, we need a model of mélange buttressed calving that is dependent on the geometries of the embayment and the ice sheet averaged over the year.

To this end, we start by assuming a linear relationship between mélange thickness and the reduction of the calving rate:

$$C = \left(1 - \frac{d}{H}\right) C^*, \tag{1}$$

where C^* is a calving rate derived for an unbuttressed glacier terminus (Morlighem et al., 2016; Mercenier et al., 2018; Schlemm and Levermann, 2019) and C is the reduced calving rate caused by mélange buttressing. H is the ice thickness at the glacier terminus and d is an effective mélange thickness comprised of the actual mélange thickness and the packing density and stiffness of the mélange (see Pollard et al. (2018)). In the absence of mélange, $d = 0$, the calving rate is not affected. As the effective mélange thickness increases, the calving rate is reduced, and at an effective mélange thickness equal to the ice thickness H, calving is completely suppressed. This could mean either that the mélange is very thick because it contains many large (potentially full-thickness) icebergs, or that it is very stiff due to frozen sea ice.

https://doi.org/10.5194/tc-2020-50
Preprint. Discussion started: 17 February 2020

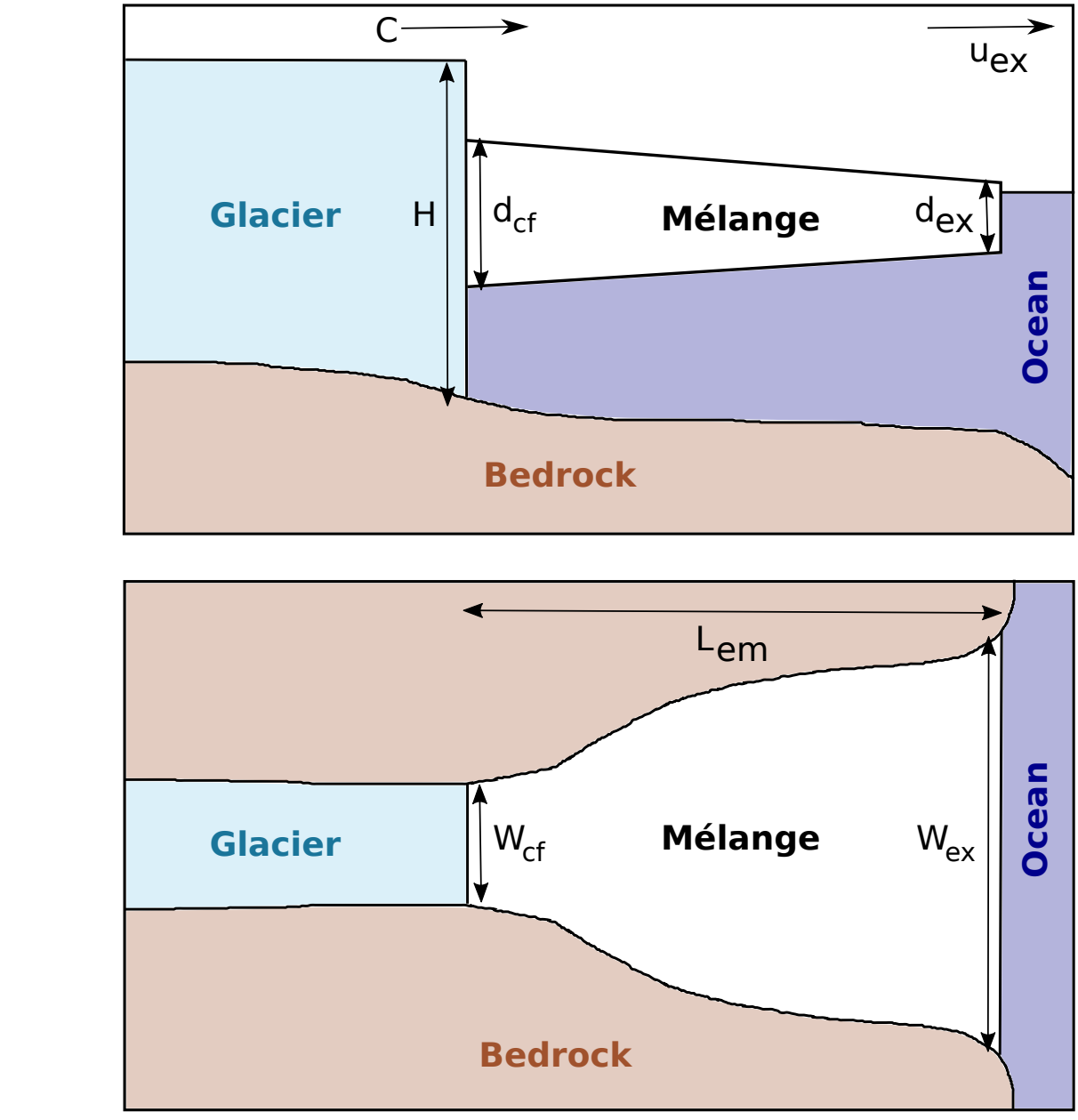

Figure 2. Geometry of the glacier terminus, ice mélange and embayment as a side view and a top view. The side view shows the ice thickness H, the calving front thickness d_{cf} and exit thickness d_{ex} of the ice mélange as well as the calving rate C and the mélange exit velocity u_{ex}. The ~~top~~ view shows the embayment width at the calving front W_{cf} and the embayment exit W_{ex} as well as the length of the embayment L_{em}.

https://doi.org/10.5194/tc-2020-50
Preprint. Discussion started: 17 February 2020

The Cryosphere Discussions

In order to estimate the effective mélange thickness d at the calving front, we assume a glacier terminating in an embayment already filled with ice mélange. Furthermore, we assume that the mélange properties are constant over the entire embayment and that the mélange thickness thins linearly along the flow direction (fig. 2).

The embayment area is given by A_{em}, its width at the calving front by W_{cf} and its width at the exit by W_{ex}. At the calving front, the glacier terminus has thickness H and is assumed to remain at a fixed position so that the calving rate C is equal to the ice flow u_{cf}. The effective mélange thickness at the calving front is given by d_{cf}. As the mélange thins on its way to the embayment exit, it has an exit thickness d_{ex} and an exit velocity u_{ex} at which mélange and icebergs are transported away by ocean currents.

We consider an effective mélange volume $V = A_{em}\bar{d}$, where $\bar{d}$ is the average effective mélange thickness. Mélange is produced at the calving front with a rate of $\mathrm{d}V/\mathrm{d}t\Big|_{cf} = W_{cf}HC$ and is lost through melting $\mathrm{d}V/\mathrm{d}t\Big|_{melt} = -mA_{em}$ (assuming constant melt rate m throughout the embayment) and by mélange exiting into the ocean $\mathrm{d}V/\mathrm{d}t\Big|_{ex} = -W_{em}d_{em}u_{ex}$. The overall rate of mélange volume is given by:

$$0 = W_{cf}HC - W_{em}d_{em}u_{ex} - mA_{em} \tag{2}$$

Assuming a steady state of mélange production and loss resulting in a constant mélange geometry, we can solve eq. 2 for d_{ex}:

$$d_{ex} = \frac{W_{cf}HC - mA_{em}}{W_{ex}u_{ex}} \tag{3}$$

This equation only has a physical solution if $mA_{em} < W_{cf}HC$, which implies that melting is small enough that mélange actually reaches the embayment exit. We assume linear thinning of the mélange along the length of the embayment such that $d_{cf} = \beta d_{ex}$ with $\beta = bL_{em}$ where b parametrizes flow properties of the mélange. Then the mélange thickness at the calving front is given as

$$d_{cf} = aCH - d_m, \qquad \text{with} \quad a = \frac{W_{cf}}{W_{ex}}\frac{bL_{em}}{u_{ex}}, \quad d_m = bL_{em}\frac{mA_{em}}{W_{ex}u_{ex}} \tag{4}$$

Inserting eq. 4 into eq. 1, we get

$$C = \left(1 + \frac{d_m}{H}\right)\frac{C^*}{1 + aC^*} \tag{5}$$

Neglecting melting we get

$$C = \frac{C^*}{1 + aC^*} = \frac{C^*}{1 + C^*/C_{max}} \tag{6}$$

This function is linear, $C \approx C^*$, for small calving rates ($C^* \ll C_{max} = a^{-1}$) and the buttressed calving C rate saturates at an upper limit $C_{max} = a^{-1}$ for large unbuttressed calving rates ($C^* \gg C_{max} = a^{-1}$). This means that the parameter a can be considered as the inverse maximum calving rate, $C_{max} = a^{-1}$, which is dependent on the embayment geometry, mélange flow properties and the embayment exit velocity. Including melt of the mélange leads to higher calving rates, because melthing thins the mélange and weakens the buttressing it gives to the calving front.

https://doi.org/10.5194/tc-2020-50
Preprint. Discussion started: 17 February 2020

Rather than imposing an upper bound on the calving rates as an ad hoc cut-off as done by DeConto and Pollard (2016); Edwards et al. (2019), mélange buttressing gives a natural upper bound on the calving rate which is reached smoothly. The value of the upper bound can be different for each glacier, depending on the embayment geometry, and may change seasonally in accord with mélange properties.

The upper limit on calving rates is a function of embayment geometry and mélange properties,

$$C_{max} = \frac{W_{ex}}{W_{cf}} \frac{u_{ex}}{\beta} \tag{7}$$

Since C_{max} is proportional to W_{ex}/W_{cf}, narrow embayments experience stronger mélange buttressing and consequently have smaller upper limits than wide open embayments. Also the longer the embayment, the smaller the upper limit, even though friction between the mélange and the embayment walls has not been taken into account. This means that for example Pine island glacier in West Antarctica will have a smaller upper bound on calving rates than neighbouring Thwaites glacier, because Pine Island lies in a valley and Thwaites glacier terminates in a wide open embayment.

3 Application to stress-based calving parametrizations

Bassis and Walker (2011) showed that ice cliffs with a glacier freeboards (ice thickness minus water depth) exceeding $\approx 100\,\mathrm{m}$ are inherently instable due to shear failure. However, smaller ice cliffs calve off icebergs as well. Mercenier et al. (2018) derived a tensile-failure based calving parametrization for calving fronts with freeboards below this stability limit, while Schlemm and Levermann (2019) derived a shear-failure based calving parametrization for calving fronts with freeboards exceeding the stability limit.

3.1 Tensile-failure based calving

A calving relation based on tensile failure was derived by Mercenier et al. (2018) who used the Hayhurst stress as failure criterion to determine the position of a large crevasse that would separate an iceberg from the glacier terminus and calculated the timescale of failure using damage propagation. The resulting tensile calving rate is given by

$$C_t^* = B \cdot \left(1 - w^{2.8}\right) \cdot \left((0.4 - 0.45(w - 0.065)^2) \cdot \rho_i g H - \sigma_{th}\right)^r \cdot H \tag{8}$$

with $B = 65$, $\sigma_{th} = 0.17$, $r = 0.43$, $\rho_i = 1020$ and $g = 9.81$. This calving relation was derived for glacier fronts with a glacier freeboard smaller than the stability limit.

3.2 Shear-failure based calving

An alternative calving relation based on shear failure of an ice cliff was derived in Schlemm and Levermann (2019), where shear failure was assumed in the lower part of an ice cliff with a freeboard larger than the stability limit. The resulting shear

https://doi.org/10.5194/tc-2020-50
Preprint. Discussion started: 17 February 2020

calving rate is given by:

$$C_s^* = C_0 \cdot \left(\frac{F - F_c}{F_s}\right)^s \tag{9}$$

$$F_s = \left(114.3\,(w - 0.3556)^4 + 20.94\right)\ \mathrm{m} \tag{10}$$

$$F_c = (75.58 - 49.18w)\ \mathrm{m} \tag{11}$$

$$s = 0.1722 \cdot \exp(2.210w) + 1.757 \tag{12}$$

with relative water depth $w \equiv D/H < 0.9$ and glacier freeboard $F \equiv H - D = H \cdot (1 - w)$. The scaling parameter C_0 is given as $C_0 = 90\,\mathrm{ma}^{-1}$, but this value is badly constrained and therefore C_0 can be considered a free parameter which parametrizes the uncertainty in the time to failure. This calving law assumes that there is no calving for freeboards smaller than the critical freeboard $F < F_c$.

Plugging the calving relation, eq. 9, into the mélange buttressed calving rate given by eq. 6 and expanding, it can be shown that the value of the upper bound C_{max} has a greater influence on the resulting calving rates than the scaling parameter C_0: Let's call the dimensionless freeboard-dependent part of the cliff calving relation

$$\tilde{C}_s = \left(\frac{F - F_c}{F_s}\right)^s, \tag{13}$$

then the buttressed calving rate is

$$C_s = \frac{\tilde{C}_s}{\frac{1}{C_0} + \frac{\tilde{C}}{C_{max}}} \tag{14}$$

Then if $1 \ll \tilde{C}$

$$C_s = C_{max} - \frac{C_{max}^2}{\tilde{C} C_0} \tag{15}$$

For small $\tilde{C}$ the choice of scaling parameter C_0 influences the final calving rate C, but for large $\tilde{C}$, the upper bound C_{max} determines the resulting calving rate. Since the scaling parameter C_0 is difficult to constrain and has little influence on the mélange buttressed calving rate, it makes sense to use a fixed value, e.g. $C_0 = 90\,\mathrm{ma}^{-1}$, and treat only the upper bound C_{max} as a free parameter (which is dependent on the embayment geometry and mélange properties).

3.3 Comparison of the calving parametrizations

A comparison of the two stress-based calving rates can be divided into four parts: Glacier fronts with very small freeboards ($<\approx 20\,\mathrm{m}$) do not calve. For glacier freeboards below the stability limit of $\approx 100\,\mathrm{m}$, there is only tensile calving with calving rates up to $\approx 10\,\mathrm{km/a}$ and no shear calving. Above the stability limit, shear calving rates increase slowly at first but speed up exponentially and equal the tensile calving rates at freeboards between $200 - 300\,\mathrm{m}$ and calving rates between $15 - 60\,\mathrm{km/a}$.

https://doi.org/10.5194/tc-2020-50
Preprint. Discussion started: 17 February 2020


The Cryosphere Discussions

There is a spread in these values because both calving rates depend on the water depth as well as the freeboard. For even larger freeboards, shear calving rates have a larger spread than tensile calving rates and much larger values for cliffs at floatation.
A comparison of the buttressed calving rates can be classified in the same way where the only difference is that large calving rates converge to a value just below the upper limit C_{max} and hence the difference between tensile and shear calving rates for large freeboards is smaller.

Summarizing, there are two different calving parametrizations, based on tensile and shear failure and derived for glacier freeboards below and above the stability limit, respectively. It might seem obvious that one should simply use each calving law in the range for which it was derived. However, that would lead to a large discontinuity in the resulting calving rate because the tensile calving rate is much larger at the stability limit than the shear calving rate. Another possibility is to use each parametrization in the range for which it gives the larger calving rate. Since it is likely that in nature large ice cliffs fail due to a combination of failure modes, it also seems reasonable to use a combination of tensile and shear calving rates.

In the context of the Marine Ice Cliff Instability (MICI) hypothesis, one would expect a sudden and large increase in calving rates for ice cliffs higher than the stability limit. Despite a nonlinear increase of calving rates in the unbuttressed case, neither of the two stress-based calving parametrizations (Mercenier et al., 2018; Schlemm and Levermann, 2019) nor a combination of them shows discontinuous behaviour at the stability limit.

3.4 Simplified calving relations

There are uncertainties in both calving laws: a dominating failure mode ~~is assumed~~ (shear and tensile failure, respectively), while in real ~~calving it is likely that~~ failure modes interact. Also, ice is assumed to be previously undamaged, whereas a glacier is usually heavily crevassed near the terminus. In addition, shear calving has a large uncertainty with respect to the time to failure which leads to uncertainty in the scaling parameter C_0. These uncertainties together with the observation that the upper limit C_{max} seems to have a stronger influence on resulting calving rates than the choice of calving law provide a good reason to consider simplifying these calving laws:
The important distinction between shear and tensile calving is that shear calving has a much larger critical freeboard: for small freeboards ($F < 100\,\mathrm{m}$), we have tensile calving but no cliff calving. Since the mélange buttressed calving rate is linear in the calving rates for small calving rates, this distinction remains in the buttressed calving rates (see fig. 3). However, for larger freeboards the calving rates approach the upper limit no matter which calving law was chosen. This distinction should be conserved in the simplified calving relations.
The dependence of the calving rate on water depth is important in the unbuttressed case (see fig. 3 on the left): there's a large range between calving rates for the same freeboard and different relative water depths – that's because larger relative water depth ~~correlates to~~ larger overall depth and hence larger ice thickness and therefore larger calving rate. But in the mélange buttressed case, the large calving rates are strongly buttressed and the large range is transformed into a much smaller range, so

https://doi.org/10.5194/tc-2020-50
Preprint. Discussion started: 17 February 2020

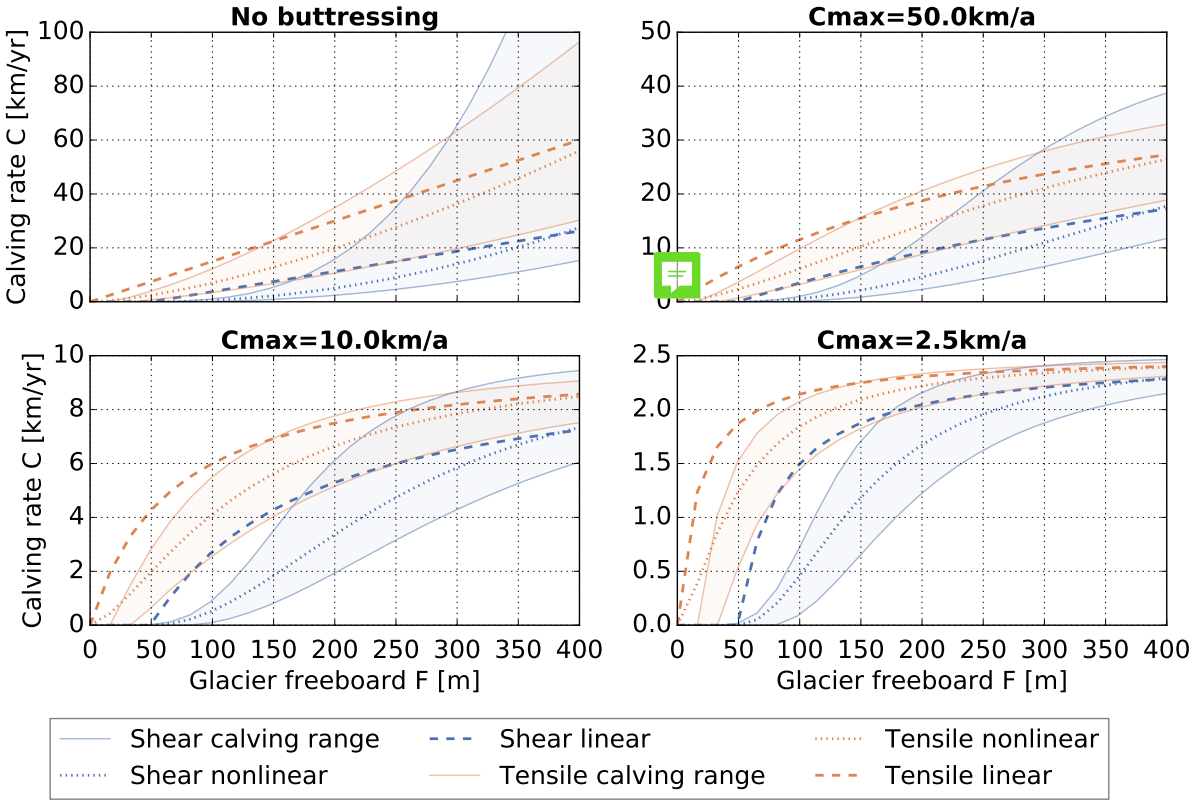

Figure 3. Calving rates as a function of glacier freeboard (ice thickness - water depth) in the unbuttressed case and for a range of upper bounds C_{max}. Shear calving and tensile calving rates depend also on the water depth: Two lines are shown for each configuration, the lower line for a dry cliff ($w = 0.0$) and the upper line for a cliff at floatatione ($w = 0.8$). This spans the range of possiible calving rates for a given freeboard. Also shown are the nonlinear (dotted line) and linear (dashed lines) approximations to these calving laws. In the tensile case, calving commences with freeboard F=0, while shear calving only happens for freeboards larger $F_c \approx 50\,\mathrm{m}$.

that water depth becomes less important.

Therefore we consider simplifications of the calving relations where we average over the water depth and further simplify:

Take the shear calving relation:

$$C_s^* = C_0 \cdot \left(\frac{F - F_c}{F_s}\right)^s \tag{16}$$

where $C_0 = 90\,\mathrm{m/a}$, $s(w) \in [1.93, 3.00]$, $F_c(w) \in [30.9, 75.0]\,\mathrm{m}$ and $F_s(w) \in [21.0, 31.1]\,\mathrm{m}$. In choosing round values within these intervals, we can simplify the relation.

$$C^*_{s,nonlin} = 90\,\mathrm{m/a} \cdot \left(\frac{F - 50\,\mathrm{m}}{20\,\mathrm{m}}\right)^2 \tag{17}$$

https://doi.org/10.5194/tc-2020-50
Preprint. Discussion started: 17 February 2020


The Cryosphere Discussions

Because the exponent s is on the smaller end of the possible values we chose a smaller value for F_s to get an approximation that lies well within the range of the full cliff calving relation, though it lies at the lower end (see fig. 3). An even simpler linear approximation

$$C^*_{s,lin} = 75\,\mathrm{a}^{-1} \cdot (F - 50\,m) \tag{18}$$

overestimates the calving rates for small freeboards ($F < 200\,\mathrm{m}$) and underestimates for large freeboards ($F > 600\,\mathrm{m}$).

The tensile calving relation can be written as

$$C^*_t = a(w)\,(b(w)F - \sigma_{th})^{0.43} \cdot F \approx c \cdot F^{1.5} \tag{19}$$

and can be fitted with a power function

$$C^*_{t,nonlin} = 7\,\mathrm{m}^{-0.5}\mathrm{a}^{-1} \cdot F^{1.5} \tag{20}$$

or a linear function

$$C^*_{t,lin} = 150\,\mathrm{a}^{-1} \cdot F \tag{21}$$

Here we neglect the small offset in freeboard that tensile calving has. This gives us two kinds of simplified calving relations to compare: one that begins calving immediately and one that only calves off cliffs larger than a certain critical freeboard. For both we have a linear approximation that overestimates small calving rates, and a nonlinear approximation that lies well within the original spread of calving rates.

4 Mélange buttressed calving in an idealized glacier setup

We consider a MISMIP3D-like glacier setup (Pattyn et al., 2013), that is symmetric ~~at~~ $x = 0$ and has periodic boundary conditions on the mountain sides. The glacial valley has an average bedrock depth of 200 m and a width of 40 km and experiences a constant accumulation of 1.5 m/a (see fig. 4). Since there is no ice reservoir at the top of the glacier, this setup can also be considered as a model for a mountain glacier.

The experiments were done with the Parallel Ice Sheet Model (PISM) (Bueler and Brown, 2009; Winkelmann et al., 2011) which uses the shallow ice approximation (Hutter, 1983) and the shallow shelf approximation (Weis et al., 1999). We use Glen's flow law in the isothermal case and a pseudoplastic basal friction law (the PISM authors, 2018).

A spin-up simulation was run until it reached a stable configuration with an attached shelf. During the experiment phase of the simulation all floating ice is removed ~~in~~ each timestep. When the shelf is removed, the marine ice sheet instability (MISI) kicks in because of the slightly retrograde bed topography and the glacier retreats. Calving accelerates this retreat. Experiments were made with no calving (MISI only), mélange buttressed shear calving and its nonlinear and linear approximation as well as mélange buttressed tensile calving and its two approximations. The upper bound was varied

https://doi.org/10.5194/tc-2020-50
Preprint. Discussion started: 17 February 2020

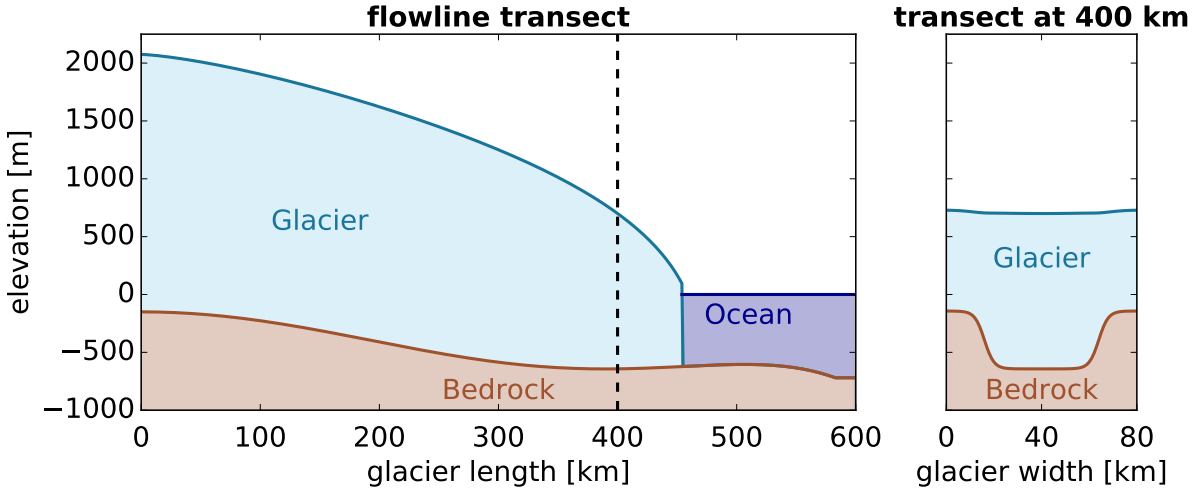

Figure 4. Setup of the idealized glacier experiments. Only one half of the setup is shown, the glacier is connected to an identical copy at the left to ensure periodic boundary conditions at the ice divide.

$C_{max} = [2.5, 20.0, 50.0, 500.0]$ km/a where the last upper bound was chosen to be large enough that the calving rates nearly match the unbuttressed calving rates.

Even without calving in the MISI only experiment, there is a significant retreat after removing the ice shelves because of the buttressing loss and slightly retrograde bed of the glacier (fig 5). The glacier retreats from a front position at 440km to 200km in the first 100 years, after which the retreat decelerates and the glacier stabilizes at a length of about 130km.

Adding calving leads to additional retreat: the higher the upper bound on the calving rates, the faster the retreat.

Shear calving causes less additional retreat than tensile calving because it has small calving rates for freeboards below 150m. Since the channel is rather shallow the freeboards are generally small. Only the linear approximation of ~~cliff~~ calving has a significant ice retreat because even though it starts only with a freeboard of 50m, it grows much faster than the actual ~~cliff~~ calving or the nonlinear approximation. But ~~it~~ also reaches a stable glacier position when the ice thickness is smaller than the critical freeboard condition.

~~Assuming~~ tensile calving~~,~~ the glacier retreat~~s~~ much faster. The linear approximation, which has higher calving rates for small freeboards, leads to a faster retreat. For the nonlinear approximation the glacier is close to floatation for most of its retreat which corresponds to the upper half of the tensile calving range. This approximation gives smaller calving rates and hence slower retreat. None of the tensile calving relations allow the glacier to stabilize. That is to say the minimum freeboard below which an ice front is stable for shear calving is ultimately the stabilizing factor in these simulations.

https://doi.org/10.5194/tc-2020-50
Preprint. Discussion started: 17 February 2020

The Cryosphere Discussions
Open Access
EGU

Fig. 6 shows that the effect of mélange buttressing becomes relevant for small values of the export of ice out of the embayment, i.e. for small values of C_{max}. In this limit of strong buttressing, i.e. where the parameterization of equation 6 is relevant, the glacier retreat becomes almost independent of the specific calving parameterization.

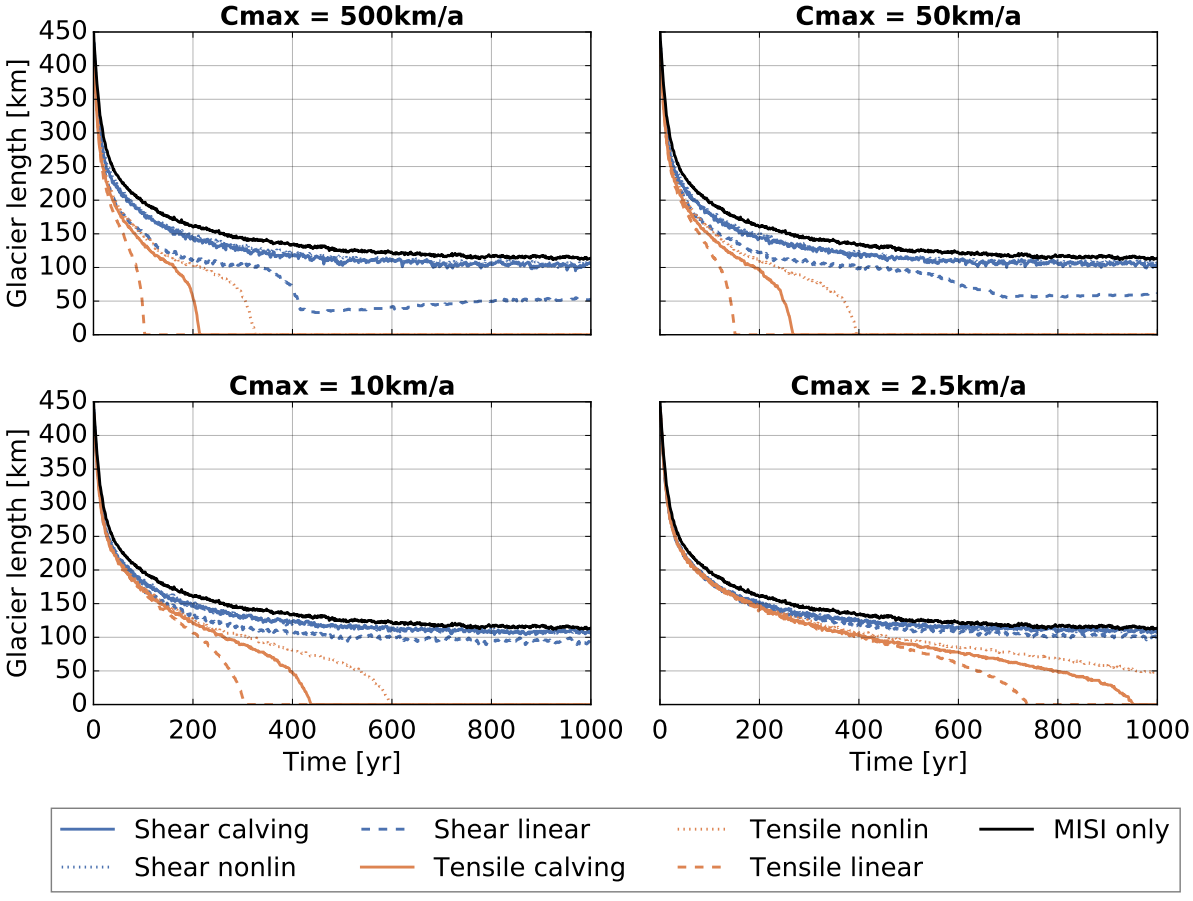

Figure 5. Glacier length timeseries. Upper left panel shows runs with an upper limit of $C_{max} = 500\,\mathrm{km/a}$ which is essentially equivalent to the unbuttressed calving rates. Then we have decreasing upper limits and consequently the glacier retreat slows down.

5 Conclusions

We considered mélange buttressing of calving glaciers as a complement to previously derived calving relations. The approach here is to provide an equation that uses simple and transparent assumptions to yield a non-trivial relation. Comparison with observations are required to support or falsify the assumption made and to calibrate the few model parameters.

The buttressing is described in form of a reduced calving rate which is a functional of the maximum calving rate as it is derived for the ice front without melange buttressing. First, we assumed that calving rates decrease linearly with the effective mélange

https://doi.org/10.5194/tc-2020-50
Preprint. Discussion started: 17 February 2020

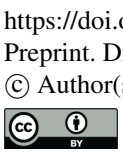

The Cryosphere Discussions
Open Access
EGU

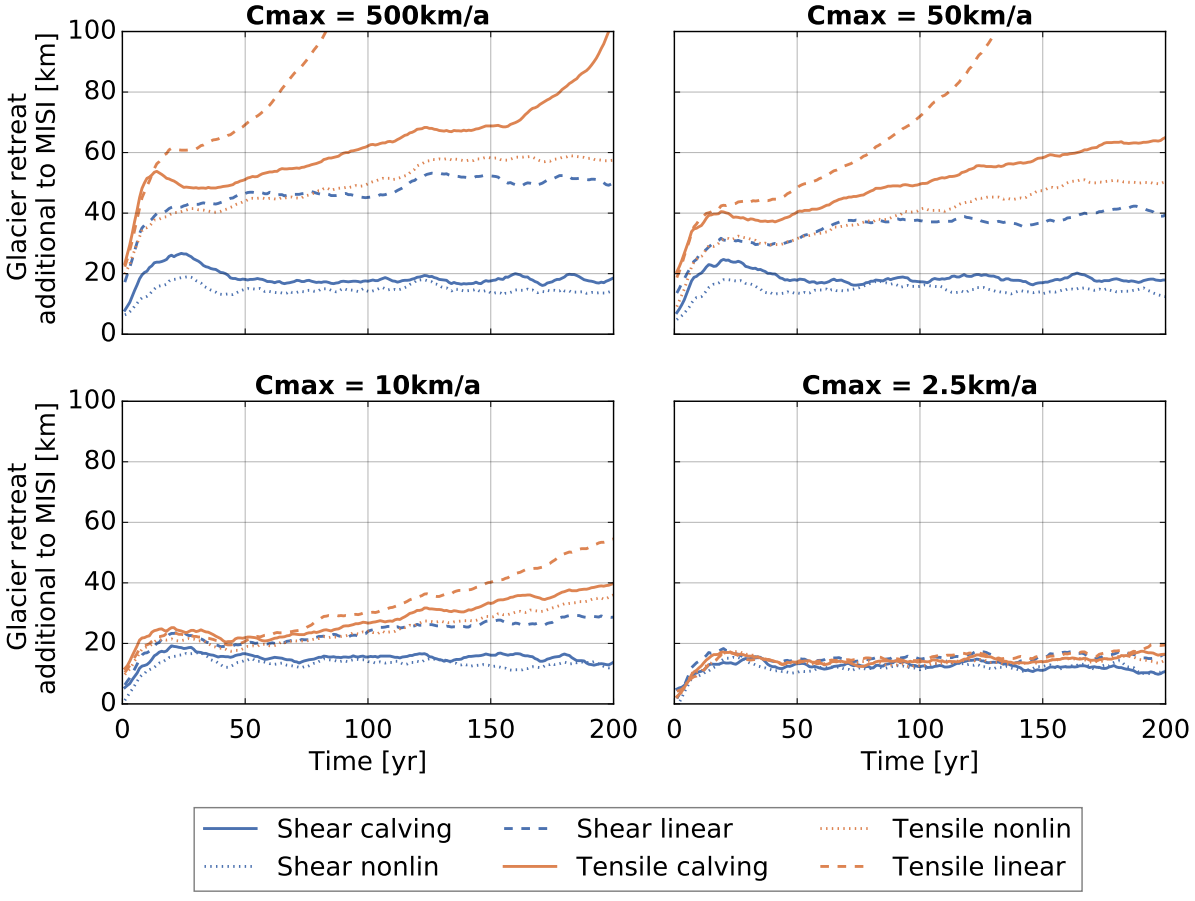

Figure 6. Timeseries of glacier retreat additional to the MISI retreat, i.e. retreat caused by calving.

thickness. The effective thickness includes stiffness and packing density of the mélange and could capture seasonal effects of increased sea ice making the mélange stiffer. Secondly, we assume a steady state between mélange production through calving and mélange loss through melting and exit from the embayment. This implies a fixed calving front position. Using these two assumptions, we derived a mélange buttressed calving rate, eq. 6, that is linear for small calving rates and converges to an upper limit, which depends on he embayment geometry, mélange flow properties and the embayment exit velocity.

This framework can be applied to any calving parametrization that gives a calving rate rather than the position of the calving front. We investigated its application to a tensile-failure based calving rate and to a shear-failure based calving rate. For small calving rates, the differences between the parametrizations persist in the buttressed case. However, large calving rates converge to the upper limit and the choice of calving parametrization becomes less important. This suggest that it is possible to simplify the calving parametrizations further, but we show that the simplifications differ for small calving rates and those differences persist.

https://doi.org/10.5194/tc-2020-50
Preprint. Discussion started: 17 February 2020

We illustrated this with a simulation of an idealized glacier. Choice of calving parametrization and choice of upper limit determine the retreat velocity.

Ocean temperatures off the coast of Antarctica are mostly sub-zero with $0.5-0.6°C$ warming expected until 2200, while the ocean temperatures off the coast of Greenland are sub-zero in the north but up to $4°C$ in the south with an expected $1.7-2.0°C$ warming until 2200 (Yin et al., 2011). This leads to increased mélange melting in Greenland compared to Antarctica and therefore higher upper limits on calving rates in Greenland glaciers that have geometries comparable to Antarctic glaciers.
Future ocean warming and intrusion of warm ocean water under the ice mélange increases melting rates and the upper limit on calving rates. This could be another mechanism by which ocean warming increases calving rates.

The concept of cliff calving and a cliff calving instability is not without criticism. According to Clerc et al. (2019), the lower part of the glacier terminus where shear failure is assumed to occur (Bassis and Walker, 2011; Schlemm and Levermann, 2019) is actually in a regime of thermal softening with a much higher critical stress and thus remains stable for large ice thicknesses. Tensile failure may occur in the shallow upper part of the cliff and initiate failure in the lower part of the cliff. The critical subaerial cliff height at which failure occurs depends on the timescale of the ice shelf collapse: for collapse times larger than 1 day, the critical cliff height lies between $(170-700\,\mathrm{m})$.

The mélange buttressing model proposed here does not depend on the specific calving mechanism and is not comprehensive especially since it is not derived from first principles but from a macroscopic perspective. The advantage of the equation proposed here is the very limited number of parameters that can be calibrated using large scale observations. Eventually a microscopic investigation of the proposed parameterization would be desirable.

Author contributions. Both authors conceived the study and analysed the data. T.S. developed the basic equations, carried out the experiments and wrote the manuscript. A.L. contributed to the writing of the manuscript.

Competing interests. No competing interests

Acknowledgements. T.S. was funded by a doctoral scholarship of the H. Boell foundation.

https://doi.org/10.5194/tc-2020-50
Preprint. Discussion started: 17 February 2020

References

Amundson, J. M., Fahnestock, M., Truffer, M., Brown, J., Lüthi, M. P., and Motyka, R. J.: Ice mélange dynamics and implications for terminus stability, Jakobshavn Isbræ, Greenland, Journal of Geophysical Research: Earth Surface, 115, https://doi.org/10.1029/2009JF001405, https://agupubs.onlinelibrary.wiley.com/doi/abs/10.1029/2009JF001405, 2010.

Bassis, J. N. and Walker, C. C.: Upper and lower limits on the stability of calving glaciers from the yield strength envelope of ice, Proceedings of the Royal Society of London A: Mathematical, Physical and Engineering Sciences, https://doi.org/10.1098/rspa.2011.0422, http://rspa.royalsocietypublishing.org/content/early/2011/11/17/rspa.2011.0422, 2011.

Bassis, J. N., Petersen, S. V., and Mac Cathles, L.: Heinrich events triggered by ocean forcing and modulated by isostatic adjustment, Nature, 542, 332, https://doi.org/10.1038/nature21069, 2017.

Benn, D. I., Hulton, N. R., and Mottram, R. H.: 'Calving laws', 'sliding laws' and the stability of tidewater glaciers, Annals of Glaciology, 46, 123–130, https://doi.org/10.3189/172756407782871161, http://www.ingentaconnect.com/content/igsoc/agl/2007/00000046/00000001/art00019, 2007.

Bueler, E. and Brown, J.: Shallow shelf approximation as a "sliding law" in a thermomechanically coupled ice sheet model, Journal of Geophysical Research: Earth Surface, 114, n/a–n/a, https://doi.org/10.1029/2008JF001179, http://dx.doi.org/10.1029/2008JF001179, 2009.

Burton, J. C., Amundson, J. M., Cassotto, R., Kuo, C.-C., and Dennin, M.: Quantifying flow and stress in ice mélange, the world's largest granular material, Proceedings of the National Academy of Sciences, 115, 5105–5110, https://doi.org/10.1073/pnas.1715136115, http://www.pnas.org/content/115/20/5105, 2018.

Church, J. A., Clark, P. U., Cazenave, A., Gregory, J. M., Jevrejeva, S., Levermann, A., Merrifield, M. A., Milne, G. A., Nerem, R. S., Nunn, P. D., Payne, A. J., Pfeffer, W. T., Stammer, D., and Unnikrishnan, A. S.: Sea-Level Rise by 2100, Science, 342, 1445–1445, https://doi.org/10.1126/science.342.6165.1445-a, http://science.sciencemag.org/content/342/6165/1445.1, 2013.

Clerc, F., Minchew, B. M., and Behn, M. D.: Marine Ice Cliff Instability Mitigated by Slow Removal of Ice Shelves, Geophysical Research Letters, 0, https://doi.org/10.1029/2019GL084183, https://agupubs.onlinelibrary.wiley.com/doi/abs/10.1029/2019GL084183, 2019.

DeConto, R. M. and Pollard, D.: Contribution of Antarctica to past and future sea-level rise, Nature, 531, 591–597, https://doi.org/http://dx.doi.org/10.1038/nature17145 10.1038/nature17145, http://www.nature.com/nature/journal/v531/n7596/abs/nature17145.html#supplementary-information, 2016.

Depoorter, M. A., Bamber, J. L., Griggs, J. A., Lenaerts, J. T. M., Ligtenberg, S. R. M., van den Broeke, M. R., and Moholdt, G.: Calving fluxes and basal melt rates of Antarctic ice shelves, Nature, 502, 89, http://dx.doi.org/10.1038/nature12567, 2013.

Edwards, T. L., Brandon, M. A., Durand, G., Edwards, N. R., Golledge, N. R., Holden, P. B., Nias, I. J., Payne, A. J., Ritz, C., and Wernecke, A.: Revisiting Antarctic ice loss due to marine ice-cliff instability, Nature, 566, 58–64, https://doi.org/10.1038/s41586-019-0901-4, 2019.

Enderlin, E. M., Howat, I. M., Jeong, S., Noh, M.-J., Angelen, J. H., and Broeke, M. R.: An improved mass budget for the Greenland ice sheet, Geophysical Research Letters, 41, 866–872, https://doi.org/10.1002/2013GL059010, https://agupubs.onlinelibrary.wiley.com/doi/abs/10.1002/2013GL059010, 2014.

Eric Rignot, Jérémie Mouginot, B. S. M. v. d. B. M. J. v. W. M. M.: Four decades of Antarctic Ice Sheet mass balance from 1979–2017, Proceedings of the National Academy of Sciences, https://doi.org/10.1073/pnas.1812883116, 2019.

Favier, L., Durand, G., Cornford, S. L., Gudmundsson, G. H., Gagliardini, O., Gillet-Chaulet, F., Zwinger, T., Payne, A. J., and Le Brocq, A. M.: Retreat of Pine Island Glacier controlled by marine ice-sheet instability, Nature Climate Change, 4, 117–121, https://doi.org/10.1038/nclimate2094, 2014.

https://doi.org/10.5194/tc-2020-50
Preprint. Discussion started: 17 February 2020

Franco, B., Fettweis, X., and Erpicum, M.: Future projections of the Greenland ice sheet energy balance driving the surface melt, The Cryosphere, 7, 1–18, https://doi.org/10.5194/tc-7-1-2013, https://www.the-cryosphere.net/7/1/2013/, 2013.

Golledge, N. R., Kowalewski, D. E., Naish, T. R., Levy, R. H., Fogwill, C. J., and Gasson, E. G. W.: The multi-millennial Antarctic commitment to future sea-level rise, Nature, 526, 421–425, https://doi.org/10.1038/nature15706, 2015.

Golledge, N. R., Keller, E. D., Gomez, N., Naughten, K. A., Bernales, J., Trusel, L. D., and Edwards, T. L.: Global environmental consequences of twenty-first-century ice-sheet melt, Nature, 566, 65–72, https://doi.org/10.1038/s41586-019-0889-9, 2019.

Hutter, K.: Theoretical Glaciology, D. Reidel Publishing Company/Terra Scientific Publishing Company, 1983.

Jeong, S., Howat, I. M., and Bassis, J. N.: Accelerated ice shelf rifting and retreat at Pine Island Glacier, West Antarctica, Geophysical Research Letters, 43, 11,720–11,725, https://doi.org/10.1002/2016GL071360, https://agupubs.onlinelibrary.wiley.com/doi/abs/10.1002/2016GL071360, 2016.

Khazendar, A., Rignot, E., and Larour, E.: Roles of marine ice, rheology, and fracture in the flow and stability of the Brunt/Stancomb-Wills Ice Shelf, Journal of Geophysical Research: Earth Surface, 114, n/a–n/a, https://doi.org/10.1029/2008JF001124, http://dx.doi.org/10.1029/2008JF001124, f04007, 2009.

Kopp, R. E., DeConto, R. M., Bader, D. A., Hay, C. C., Horton, R. M., Kulp, S., Oppenheimer, M., Pollard, D., and Strauss, B. H.: Evolving Understanding of Antarctic Ice-Sheet Physics and Ambiguity in Probabilistic Sea-Level Projections, Earth's Future, 5, 1217–1233, https://doi.org/10.1002/2017EF000663, https://agupubs.onlinelibrary.wiley.com/doi/abs/10.1002/2017EF000663, 2017.

Krug, J., Durand, G., Gagliardini, O., and Weiss, J.: Modelling the impact of submarine frontal melting and ice mélange on glacier dynamics, The Cryosphere, 9, 989–1003, https://doi.org/10.5194/tc-9-989-2015, https://www.the-cryosphere.net/9/989/2015/, 2015.

Levermann, A. and Winkelmann, R.: A simple equation for the melt elevation feedback of ice sheets, The Cryosphere, 10, 1799–1807, https://doi.org/10.5194/tc-10-1799-2016, https://www.the-cryosphere.net/10/1799/2016/, 2016.

Levermann, A., Albrecht, T., Winkelmann, R., Martin, M. A., Haseloff, M., and Joughin, I.: Kinematic first-order calving law implies potential for abrupt ice-shelf retreat, The Cryosphere, 6, 273–286, https://doi.org/10.5194/tc-6-273-2012, http://www.the-cryosphere.net/6/273/2012/, 2012.

Levermann, A., Winkelmann, R., Albrecht, T., Goelzer, H., Golledge, N. R., Greve, R., Huybrechts, P., Jordan, J., Leguy, G., Martin, D., Morlighem, M., Pattyn, F., Pollard, D., Quiquet, A., Rodehacke, C., Seroussi, H., Sutter, J., Zhang, T., Van Breedam, J., DeConto, R., Dumas, C., Garbe, J., Gudmundsson, G. H., Hoffman, M. J., Humbert, A., Kleiner, T., Lipscomb, W., Meinshausen, M., Ng, E., Perego, M., Price, S. F., Saito, F., Schlegel, N.-J., Sun, S., and van de Wal, R. S. W.: Projecting Antarctica's contribution to future sea level rise from basal ice-shelf melt using linear response functions of 16 ice sheet models (LARMIP-2), Earth System Dynamics Discussions, 2019, 1–63, https://doi.org/10.5194/esd-2019-23, https://www.earth-syst-dynam-discuss.net/esd-2019-23/, 2019.

Mengel, M., Feldmann, J., and Levermann, A.: Linear sea-level response to abrupt ocean warming of major West Antarctic ice basin, Nature Climate Change, 6, 71, http://dx.doi.org/10.1038/nclimate2808, 2016.

Mercenier, R., Lüthi, M. P., and Vieli, A.: Calving relation for tidewater glaciers based on detailed stress field analysis, The Cryosphere, 12, 721–739, https://doi.org/10.5194/tc-12-721-2018, https://www.the-cryosphere.net/12/721/2018/, 2018.

Mercer, J. H.: West Antarctic ice sheet and CO2 greenhouse effect: a threat of disaster, Nature, 271, 321–325, https://doi.org/10.1038/271321a0, 1978.

Morlighem, M., Bondzio, J., Seroussi, H., Rignot, E., Larour, E., Humbert, A., and Rebuffi, S.: Modeling of Store Gletscher's calving dynamics, West Greenland, in response to ocean thermal forcing, Geophysical Research Letters, 43, 2659–2666, https://doi.org/10.1002/2016GL067695, http://dx.doi.org/10.1002/2016GL067695, 2016GL067695, 2016.

https://doi.org/10.5194/tc-2020-50
Preprint. Discussion started: 17 February 2020

Mouginot, J., Rignot, E., Bjørk, A. A., van den Broeke, M., Millan, R., Morlighem, M., Noël, B., Scheuchl, B., and Wood, M.: Forty-six years of Greenland Ice Sheet mass balance from 1972 to 2018, Proceedings of the National Academy of Sciences, 116, 9239–9244, https://doi.org/10.1073/pnas.1904242116, https://www.pnas.org/content/116/19/9239, 2019.

Nick, F., van der Veen, C., Vieli, A., and Benn, D.: A physically based calving model applied to marine outlet glaciers and implications for the glacier dynamics, Journal of Glaciology, 56, 781–794, https://doi.org/doi:10.3189/002214310794457344, http://www.ingentaconnect.com/content/igsoc/jog/2010/00000056/00000199/art00004, 2010.

Pattyn, F., Perichon, L., Durand, G., Favier, L., Gagliardini, O., Hindmarsh, R. C., Zwinger, T., Albrecht, T., Cornford, S., Docquier, D., and et al.: Grounding-line migration in plan-view marine ice-sheet models: results of the ice2sea MISMIP3d intercomparison, Journal of Glaciology, 59, 410–422, https://doi.org/10.3189/2013JoG12J129, 2013.

Pollard, D., DeConto, R. M., and Alley, R. B.: Potential Antarctic Ice Sheet retreat driven by hydrofracturing and ice cliff failure, Earth and Planetary Science Letters, 412, 112 – 121, https://doi.org/http://dx.doi.org/10.1016/j.epsl.2014.12.035, http://www.sciencedirect.com/science/article/pii/S0012821X14007961, 2015.

Pollard, D., DeConto, R. M., and Alley, R. B.: A continuum model of ice mélange and its role during retreat of the Antarctic Ice Sheet, Geoscientific Model Development Discussions, 2018, 1–38, https://doi.org/10.5194/gmd-2018-28, https://www.geosci-model-dev-discuss.net/gmd-2018-28/, 2018.

Rignot, E. and Kanagaratnam, P.: Changes in the Velocity Structure of the Greenland Ice Sheet, Science, 311, 986–990, https://doi.org/10.1126/science.1121381, http://science.sciencemag.org/content/311/5763/986, 2006.

Rignot, E. and MacAyeal, D. R.: Ice-shelf dynamics near the front of the Filchner—Ronne Ice Shelf, Antarctica, revealed by SAR interferometry, Journal of Glaciology, 44, 405–418, https://doi.org/10.3189/S0022143000002732, 1998.

Rignot, E., Mouginot, J., Morlighem, M., Seroussi, H., and Scheuchl, B.: Widespread, rapid grounding line retreat of Pine Island, Thwaites, Smith, and Kohler glaciers, West Antarctica, from 1992 to 2011, Geophysical Research Letters, 41, 3502–3509, https://doi.org/10.1002/2014GL060140, http://dx.doi.org/10.1002/2014GL060140, 2014.

Ritz, C., Edwards, Tamsin L., Durand, Gaël, Payne, Antony J., Peyaud, Vincent, and Hindmarsh, Richard C. A.: Potential sea-level rise from Antarctic ice-sheet instability constrained by observations, Nature, 528, 115–118, https://doi.org/http://dx.doi.org/10.1038/nature16147 10.1038/nature16147, http://www.nature.com/nature/journal/v528/n7580/abs/nature16147.html#supplementary-information, 2015.

Schlemm, T. and Levermann, A.: A simple stress-based cliff-calving law, The Cryosphere, 13, 2475–2488, https://doi.org/10.5194/tc-13-2475-2019, https://www.the-cryosphere.net/13/2475/2019/, 2019.

Schoof, C.: Ice sheet grounding line dynamics: Steady states, stability, and hysteresis, Journal of Geophysical Research: Earth Surface, 112, n/a–n/a, https://doi.org/10.1029/2006JF000664, http://dx.doi.org/10.1029/2006JF000664, f03S28, 2007.

Shepherd, A., Ivins, E., Rignot, E., Smith, B., van den Broeke, M., Velicogna, I., Whitehouse, P., Briggs, K., Joughin, I., Krinner, G., Nowicki, S., Payne, T., Scambos, T., Schlegel, N., Geruo, A., Agosta, C., Ahlstrøm, A., Babonis, G., Barletta, V., Blazquez, A., Bonin, J., Csatho, B., Cullather, R., Felikson, D., Fettweis, X., Forsberg, R., Gallee, H., Gardner, A., Gilbert, L., Groh, A., Gunter, B., Hanna, E., Harig, C., Helm, V., Horvath, A., Horwath, M., Khan, S., Kjeldsen, K. K., Konrad, H., Langen, P., Lecavalier, B., Loomis, B., Luthcke, S., McMillan, M., Melini, D., Mernild, S., Mohajerani, Y., Moore, P., Mouginot, J., Moyano, G., Muir, A., Nagler, T., Nield, G., Nilsson, J., Noel, B., Otosaka, I., Pattle, M. E., Peltier, W. R., Pie, N., Rietbroek, R., Rott, H., Sandberg-Sørensen, L., Sasgen, I., Save, H., Scheuchl, B., Schrama, E., Schröder, L., Seo, K.-W., Simonsen, S., Slater, T., Spada, G., Sutterley, T., Talpe, M., Tarasov, L., van de Berg, W. J., van der Wal, W., van Wessem, M., Vishwakarma, B. D., Wiese, D., Wouters, B., and team, T. I. M. B. I. E.: Mass balance of the Antarctic Ice Sheet from 1992 to 2017, Nature, 558, 219–222, https://doi.org/10.1038/s41586-018-0179-y, 2018.

https://doi.org/10.5194/tc-2020-50
Preprint. Discussion started: 17 February 2020

Slangen, A. B. A., Adloff, F., Jevrejeva, S., Leclercq, P. W., Marzeion, B., Wada, Y., and Winkelmann, R.: A Review of Recent Updates of Sea-Level Projections at Global and Regional Scales, pp. 395–416, Springer International Publishing, Cham, https://doi.org/10.1007/978-3-319-56490-6_17, https://doi.org/10.1007/978-3-319-56490-6_17, 2017.

the PISM authors: PISM, a Parallel Ice Sheet Model, https://pism-docs.org, 2018.

Todd, J. and Christoffersen, P.: Are seasonal calving dynamics forced by buttressing from ice mélange or undercutting by melting? Outcomes from full-Stokes simulations of Store Glacier, West Greenland, The Cryosphere, 8, 2353–2365, https://doi.org/10.5194/tc-8-2353-2014, https://www.the-cryosphere.net/8/2353/2014/, 2014.

Todd, J., Christoffersen, P., Zwinger, T., Råback, P., Chauché, N., Benn, D., Luckman, A., Ryan, J., Toberg, N., Slater, D., and Hubbard, A.: A Full-Stokes 3-D Calving Model Applied to a Large Greenlandic Glacier, Journal of Geophysical Research: Earth Surface, 123, 410–432, https://doi.org/10.1002/2017JF004349, https://agupubs.onlinelibrary.wiley.com/doi/abs/10.1002/2017JF004349, 2018.

Todd, J., Christoffersen, P., Zwinger, T., Råback, P., and Benn, D. I.: Sensitivity of a calving glacier to ice–ocean interactions under climate change: new insights from a 3-D full-Stokes model, The Cryosphere, 13, 1681–1694, https://doi.org/10.5194/tc-13-1681-2019, https://www.the-cryosphere.net/13/1681/2019/, 2019.

Walter, J. I., Box, J. E., Tulaczyk, S., Brodsky, E. E., Howat, I. M., Ahn, Y., and Brown, A.: Oceanic mechanical forcing of a marine-terminating Greenland glacier, Annals of Glaciology, 53, 181–192, https://doi.org/10.3189/2012AoG60A083, 2012.

WCRP Global Sea Level Budget Group: Global sea-level budget 1993–present, Earth System Science Data, 10, 1551–1590, https://doi.org/10.5194/essd-10-1551-2018, https://www.earth-syst-sci-data.net/10/1551/2018/, 2018.

Weis, M., Greve, R., and Hutter, K.: Theory of shallow ice shelves, Continuum Mechanics and Thermodynamics, 11, 15–50, https://doi.org/10.1007/s001610050102, https://doi.org/10.1007/s001610050102, 1999.

Winkelmann, R., Martin, M. A., Haseloff, M., Albrecht, T., Bueler, E., Khroulev, C., and Levermann, A.: The Potsdam Parallel Ice Sheet Model (PISM-PIK) – Part 1: Model description, The Cryosphere, 5, 715–726, https://doi.org/10.5194/tc-5-715-2011, http://www.the-cryosphere.net/5/715/2011/, 2011.

Xie, S., Dixon, T. H., Holland, D. M., Voytenko, D., and Vaňková, I.: Rapid iceberg calving following removal of tightly packed pro-glacial mélange, Nature Communications, 10, 3250, https://doi.org/10.1038/s41467-019-10908-4, 2019.

Yin, J., Overpeck, J. T., Griffies, S. M., Hu, A., Russell, J. L., and Stouffer, R. J.: Different magnitudes of projected subsurface ocean warming around Greenland and Antarctica, Nature Geoscience, 4, 524–528, https://doi.org/10.1038/ngeo1189, 2011.